

# Development of an empirical correlation for predicting shear wave velocity of Christchurch soils from cone penetration test data



Christopher R. McGann<sup>a,\*</sup>, Brendon A. Bradley<sup>b</sup>, Merrick L. Taylor<sup>b</sup>,  
Liam M. Wotherspoon<sup>c</sup>, Misko Cubrinovski<sup>b</sup>

<sup>a</sup> Department of Civil and Environmental Engineering, Washington State University, PO Box 642910, Pullman, WA 99194, USA

<sup>b</sup> Department of Civil and Natural Resources Engineering, University of Canterbury, Private Bag 4800, Christchurch, New Zealand

<sup>c</sup> Department of Civil and Environmental Engineering, The University of Auckland, Private Bag 92019, Auckland, New Zealand

## ARTICLE INFO

### Article history:

Received 15 April 2014

Received in revised form

10 February 2015

Accepted 27 March 2015

Available online 22 April 2015

### Keywords:

Cone penetration test (CPT)

Shear wave velocity

Multiple linear regression

Seismic piezocone (SCPTu)

Empirical correlation

## ABSTRACT

Following the companion study of McGann et al. [1], seismic piezocone (SCPTu) data compiled from sites in Christchurch, New Zealand area are used with multiple linear regression to develop a Christchurch-specific empirical correlation for use in predicting soil shear wave velocities,  $V_s$ , from cone penetration test (CPT) data. An appropriate regression functional form is selected through an evaluation of the residuals for regression models developed with the Christchurch SCPTu database using functional forms adopted by previous empirical correlations between  $V_s$  and CPT data. An examination of how the residuals for the chosen regression form vary with the predictor variables identifies the need for non-constant depth variance in the regression model. The performance of the model is assessed through comparisons of predicted and observed  $V_s$  profiles and through forward predictions with synthetic CPT data. The new CPT– $V_s$  correlation provides a method to estimate  $V_s$  from CPT data that is specific to the non-gravel soils of the Christchurch region in their current state (caution should be used for western portions of the Springston Formation where SCPTu data were sparse). The correlation also enables the utilization of the large, high-density database of CPT logs ( $> 15,000$  as of 1/1/2014) in the Christchurch region for the development of both site-specific and region-wide models of surficial  $V_s$  for use in site characterization and site response analysis.

© 2015 Elsevier Ltd. All rights reserved.

## 1. Introduction

Site effects related to the influence of near-surface ( $< 50$  m) stratigraphy strongly affect observed surficial ground motions. Seismic waves must always pass through these near-surface soil and rock layers before reaching the surface, thus site effects tend to be a systematic feature of observed ground motions at a particular location, while path and source effects, which also strongly affect surficial ground motions, can vary significantly for earthquakes originating from different sources. The systematic nature of site effects at a particular site, in combination with the ready availability of direct measurements and estimates of the characteristics and properties of the near-surface soils, indicates that local site effects can be modelled with potentially greater accuracy than source and path effects and, therefore, offer a

potentially more efficient means with which to predict the character, and effects, of future surficial ground motions at specific locations [2–5].

The small strain shear modulus is a fundamental parameter required to evaluate the dynamic response of soil deposits using seismic site response analysis. It defines the shear stress–strain response for low levels of strain ( $< 10^{-4}\%$ ), and is typically used to define normalized relationships describing the reduction in soil shear modulus with increasing levels of strain that is critical to nonlinear and equivalent linear site response analyses (e.g. [6,7]). The small strain shear modulus is highly susceptible to disturbances that are nearly unavoidable in any laboratory assessment [8], therefore, in situ measurements or estimates of shear wave velocity,  $V_s$ , which is related to the small strain shear modulus through the linear elastic wave propagation equation, are used to obtain the low strain soil shear modulus profiles necessary for dynamic site response analyses.

Near surface shear wave velocities can be directly estimated using surface wave measurement techniques such as the spectral and multi-channel analysis of surface waves techniques (SASW and MASW, respectively) [9,10], linear and microtremor array methods [11–14], as well as by techniques requiring one or more

\* Corresponding author. Tel.: +1 509 335 7320.

E-mail addresses: [christopher.mcgann@wsu.edu](mailto:christopher.mcgann@wsu.edu) (C.R. McGann),  
[brendon.bradley@canterbury.ac.nz](mailto:brendon.bradley@canterbury.ac.nz) (B.A. Bradley),  
[merrick.taylor@pg.canterbury.ac.nz](mailto:merrick.taylor@pg.canterbury.ac.nz) (M.L. Taylor),  
[l.wotherspoon@auckland.ac.nz](mailto:l.wotherspoon@auckland.ac.nz) (L.M. Wotherspoon),  
[misko.cubrinovski@canterbury.ac.nz](mailto:misko.cubrinovski@canterbury.ac.nz) (M. Cubrinovski).

boreholes such as crosshole and downhole techniques [15,16] and P-S suspension logging measurements [17]. Near surface  $V_s$  profiles can also be obtained via empirical correlations with common geotechnical investigations such as the standard penetration test (SPT) (e.g. [18–21]) and the cone penetration test (CPT) (e.g. [19,21–27]). Such empirical correlations are typically developed through regression analysis using a series of predictor variables from the conventional geotechnical investigations (SPT or CPT) and  $V_s$  measurements obtained through one of the previously mentioned techniques. Many of the more recent empirical correlations have been developed using data for general soil deposits (i.e., cohesive and cohesionless) from globally located sites of varying geological ages in order to obtain prediction correlations that can be applied in a general manner.

Direct in situ  $V_s$  measurements are preferable to the indirect  $V_s$  estimations obtained from the application of empirical correlations, however, they have disadvantages that limit their use in general practice. Surface wave methods are useful in that they are generally non-intrusive, but they require the solution of an inverse problem, which is often ill-posed. As a result,  $V_s$  profiles estimated using surface wave techniques often have problems related to the non-uniqueness of the solution [28] and to the equivalence problem [11,29]. These issues can be manifested in the resulting profiles via decreased resolution with increasing depth, an inability to identify thin layers, and difficulties in resolving the portions of layers adjacent to large velocity contrasts [8]. Borehole-type measurement techniques are inherently invasive, though this in itself does not preclude their use, as invasive site characterization techniques (e.g. SPT and CPT) are common in practice. Compared to surface wave methods, borehole-type measurement techniques have greater capacity to resolve inclusions and anomalies that may be missed by surface-based approaches, but have increased temporal and financial expenses associated with drilling (especially for crosshole techniques, which require multiple boreholes) [8], and only represent the subsurface conditions at a single point, rather than the conditions averaged along a line. The downhole technique, of which the seismic cone penetration test (SCPT) is a specialized subset, requires only a single borehole, but can suffer from depth limits depending on the energy of the seismic wave source. The suspension logger test can be used for great depths (> 100 m), and is arguably the most precise invasive measurement method currently available, but this test has limited application in soft sediments [8].

The noted difficulties associated with direct  $V_s$  measurement techniques, along with the expenses related to the specialized equipment and training associated with their use in practice, typically results in their use only at certain higher-importance sites and a corresponding scarcity of  $V_s$  data available for region-wide subsurface characterization. In contrast, site investigation techniques such as SPT and CPT are commonly applied to a broader scope of projects, and empirical correlations based on the data obtained by such tests can be used to provide the  $V_s$  data necessary for both region-wide and site-specific ground response assessments. This is especially true in Christchurch, where the extensive site investigations made following the 2010–2011 Canterbury earthquake sequence [2,30–34] have resulted in a large, high density database of CPT logs (> 15,000 as of 1/1/2014) for sites located throughout Christchurch and the surrounding suburbs and towns.

This paper presents the development of an empirical correlation between CPT data and soil  $V_s$ . The paper extends on McGann et al. [1] who used a SCPTu database obtained from 86 sites in the greater Christchurch, New Zealand area to evaluate the suitability of four existing empirical models for estimating the in situ  $V_s$  of Christchurch soils from CPT data. The existing CPT– $V_s$  correlations [22–24] were shown to be biased towards overestimating the

observed  $V_s$  profiles on average, with the Andrus et al. [22] correlation providing the predictions with the least amount of prediction error. Reduction or loss of age effects was presented as one of the possible reasons for the observed overestimation bias in the existing correlations when applied to Christchurch soils, as the examined Christchurch sites do not display an increase in  $V_s$  with effective deposit age in line with that displayed by the existing Andrus et al. [22] data set. The observations discussed in McGann et al. [1] demonstrated the need for the development of a new Christchurch-specific CPT– $V_s$  correlation through regression analysis, and this development is discussed in the current paper. Firstly, the development focuses on the selection of an appropriate functional form for the regression analysis. Secondly, the quality of the regression using the selected functional form is assessed, with particular attention given to the dependence of the model prediction and standard deviation on various predictor variables, and also direct comparison for selected profiles. The details of the correlation development are presented in the ensuing sections, followed by a discussion of the recommended Christchurch-specific CPT– $V_s$  correlation determined through this process.

## 2. Evaluation of regression function forms

The first step in the development of a regression between CPT data and  $V_s$  is an assessment of potential functional forms. McGann et al. [1] examined the predictive capabilities of several existing CPT– $V_s$  correlations to SCPTu data from the Christchurch region, and the functional forms of the those examined relationships form the basis of those considered herein. Specifically, six distinct relations between  $V_s$  and various CPT-based variables are considered as candidate regression functions. The considered regression forms include the Andrus et al. [22] form

$$V_s = a q_t^b I_c^d z^e \quad (1)$$

where  $a$ ,  $b$ ,  $d$ , and  $e$  are regression coefficients,  $q_t$  is the cone tip resistance corrected for pore pressures acting behind the cone tip [35],  $I_c$  is the soil behaviour type index [36], and  $z$  is the depth; the Hegazy and Mayne [23] form rearranged to solve for shear wave velocity

$$V_s = a Q_{tn} \exp(b I_c) \left( \frac{\sigma'_{v0}}{p_a} \right)^{0.25} \quad (2)$$

where  $Q_{tn}$  is the normalized cone resistance [36,37],  $\sigma'_{v0}$  is vertical effective stress, and  $p_a$  is atmospheric pressure; the Robertson [24] form

$$V_s = \left[ 10^{a+b I_c} \left( \frac{q_t - \sigma_{v0}}{p_a} \right) \right]^{0.5} \quad (3)$$

in which all terms are previously defined; the form recommended for use in CPT– $V_s$  regression analysis by Wair et al. [21]

$$V_s = a q_t^b f_s^c \sigma_{v0}^e \quad (4)$$

where  $f_s$  is the cone frictional resistance; and two additional hybrid forms that consider different combinations of terms from the forms in Eqs. (1) and (4) are

$$V_s = a q_t^b f_s^d z^e \quad (5)$$

$$V_s = a q_t^b I_c^d \sigma_{v0}^e \quad (6)$$

Multiple linear regression in logarithmic space is used with the Christchurch SCPTu data set for each of the six considered regression forms. Fig. 1 shows a comparison between the measured  $V_s$  values from the database and the  $V_s$  values estimated using each considered regression form (indicated by equation number). The plots and associated coefficients of determination,

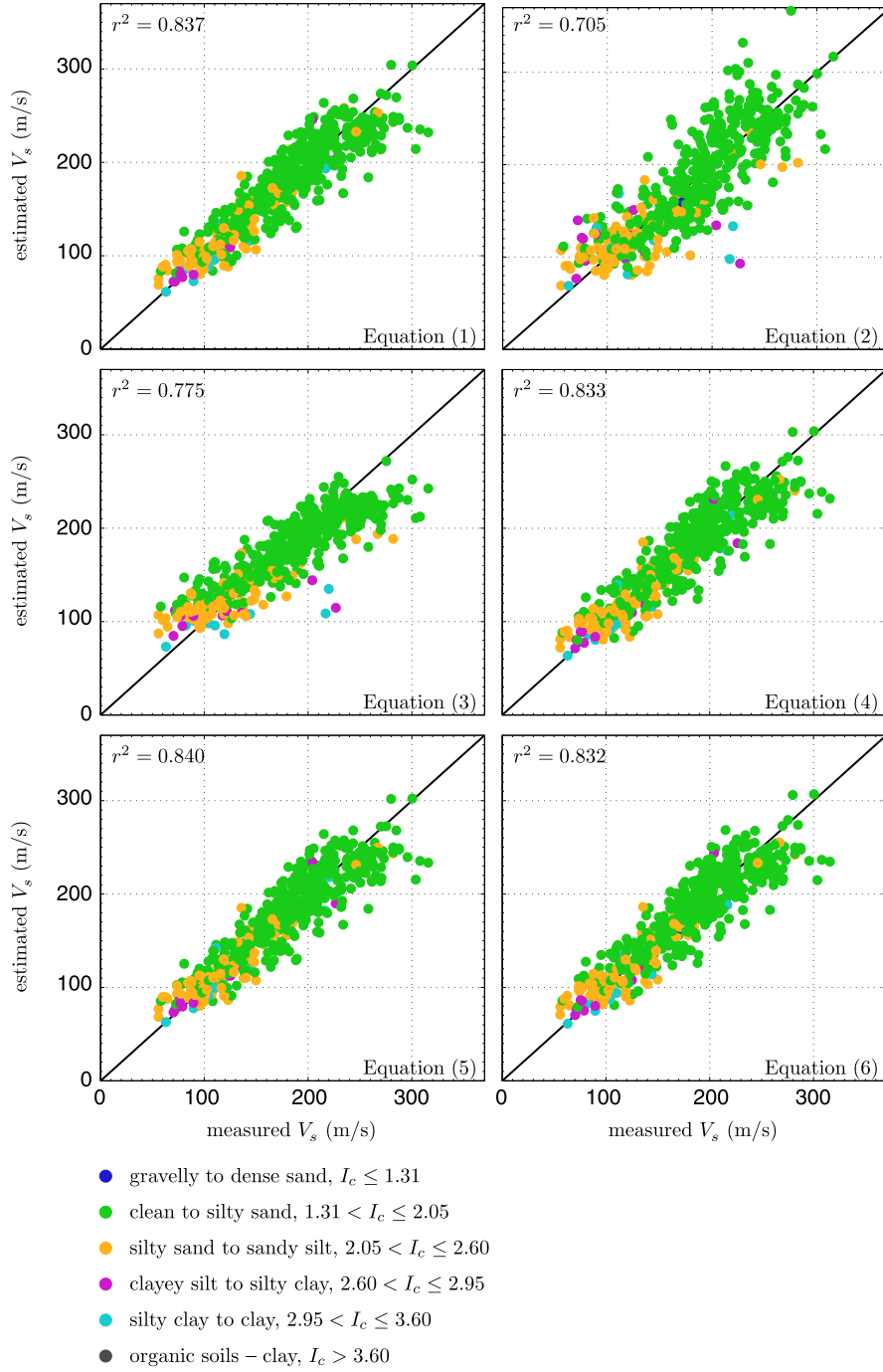


**Fig. 1.** Comparison of estimated and measured  $V_s$  for indicated regression functional forms. Marker colour indicates the  $I_c$  soil behaviour type index of the data points as noted. (For interpretation of the references to colour in this figure caption, the reader is referred to the web version of this paper.)

$r^2$ , shown in Fig. 1 indicate the relative compatibility of each regression form to the current data set. Based on these results, the Hegazy and Mayne [23] and Robertson [24] forms, Eqs. (2) and (3), respectively, appear to be the least applicable to the Christchurch data set, while the remaining four polynomial-based forms all provide a similar representation of the measured data.

The residuals for the fitted regression lines provide another means of evaluating the various regression forms. To this purpose, the residuals,  $\varepsilon$ , are defined as

$$\varepsilon = \frac{\ln(y_i) - \ln(\bar{y}_i)}{S_{Y|X}} \quad (7)$$

where  $\ln(\odot)$  is the natural logarithm function,  $y_i$  are the measured  $V_s$  values,  $\bar{y}_i$  are the  $V_s$  values returned by the regression lines, and  $S_{Y|X}$  is an estimate of the conditional standard deviation (e.g. [38, pp. 306–325]):

$$S_{Y|X} = \sqrt{\frac{\sum (\ln(y_i) - \ln(\bar{y}_i))^2}{n - 4}} \quad (8)$$

where  $n=513$  is the number of data pairs included in the regression. Fig. 2 shows how the computed residuals vary with the depth,  $z$ , of the SCPTu data set, which showed the largest variation in residuals of the considered CPT variables. Plots

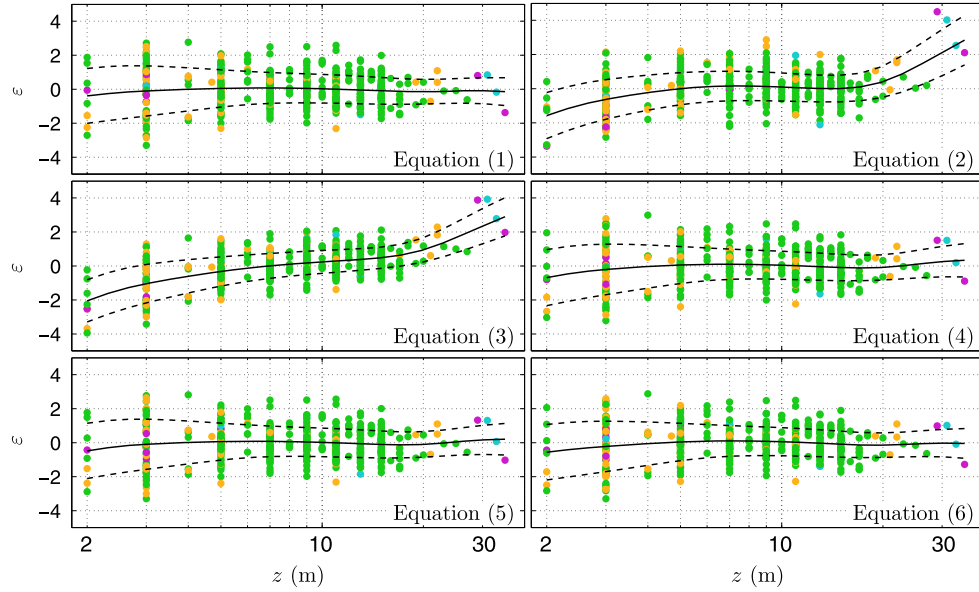


**Fig. 2.** Variation of residuals with depth,  $z$ , for indicated regression forms. Marker colour indicates the  $I_c$  soil behaviour type index of the data points as noted in Fig. 1. (For interpretation of the references to colour in this figure caption, the reader is referred to the web version of this paper.)

showing the variation of the residuals with the remaining CPT-based variables,  $q_c$ ,  $f_s$ ,  $z$ , estimated  $V_s$ , and  $I_c$ , are available in McGann et al. [39]. The marker colours in Fig. 2 represent the soil behaviour type index of each data point as indicated, while the black lines represent the moving averages (solid line) with 95% confidence intervals (dashed lines) (e.g. [40]) for the residuals.

As shown in Fig. 2, the regression forms given by Eqs. (1), (4), (5), and (6), the first two of which are the forms of Andrus et al. [22] and Wair et al. [21], respectively, produce reasonably consistent, and nearly identical, residual distributions across the range of depths in the database. In contrast, Eqs. (2) and (3), the Hegazy and Mayne [23] and Robertson [24] functional forms, display regions of concentrated bias, tend to overestimate the measured  $V_s$  data at shallow ( $z < 4$  m) locations and underestimate the data at deeper locations ( $z > 20$  m). The residual variation plots for the other CPT variables (not shown here, see [39]) show similar trends to those demonstrated in Fig. 2; the regression functional forms of Eqs. (2) and (3) return residuals that are biased towards under- or over-prediction of the measured  $V_s$  for certain ranges of  $q_c$ ,  $f_s$ , estimated  $V_s$ , and  $I_c$ , while the remaining four regression forms produce residual distributions that are similar in form and consistent across the CPT-based variable ranges in the Christchurch-specific data set.

After ruling out the regression forms of Eqs. (2) and (3), the selection criteria for the most applicable functional form becomes more subtle. As shown in Figs. 1 and 2, the differences between the  $V_s$  estimates provided by the four remaining regression forms, Eqs. (1), (4), (5), and (6), are practically negligible over the principal ranges of the data set. Given this similarity in performance, consideration for the predictor variables included in the regression equations and how these variables affect the use of the resulting correlation becomes important. The first distinguishing characteristic between these four functional forms is the use of depth,  $z$ , or initial vertical effective stress,  $\sigma'_{v0}$ , as an indicator for the state of stress in the soil. From a theoretical standpoint,  $\sigma'_{v0}$  is preferable, however, from a practical standpoint, depth may be a better choice. For a given site and CPT record, the depth is an inherently known quantity, while  $\sigma'_{v0}$  is typically estimated based on assumptions of soil mass density and groundwater table depth, and errors or uncertainties in estimated values for density, water table depth, and  $\sigma'_{v0}$  could lead to less reliable  $V_s$  predictions. This distinction is

somewhat supported by the  $r^2$  values provided in Fig. 1, which are slightly larger for the regression forms that consider depth, Eqs. (1) and (5), instead of effective stress, Eqs. (4) and (6).

The second decision relates to the use of  $f_s$  or  $I_c$ , as these terms are the only differences between the remaining two regression forms, Eqs. (1) and (5). Since each functional form appears to be equally applicable to the Christchurch data set by the measures presented here, the form given in Eq. (5) is chosen due to its use of  $f_s$ , which is directly measured by the CPT, instead of  $I_c$ , which is a computed variable (function of  $q_c$ ,  $f_s$ , and depth). While  $I_c$  is a commonly used indicator of soil behaviour type that carries useful connotations for many geotechnical engineers, its computation requires an additional step not required by  $f_s$  and its use in the CPT- $V_s$  correlation may lead to erroneous predictions due to various available presentations of the  $I_c$  function or soil behaviour type zones (e.g. [36,41,42]).

It is also of interest to assess the effects of consideration for the raw cone tip resistance,  $q_c$ , instead of the pore pressure corrected tip resistance,  $q_t$ . As shown in Fig. 3, there is effectively zero difference in the quality of the regression when consideration is made for the raw cone resistance. The  $V_s$  values estimated using  $q_c$  as a predictor variable differ from those estimated using  $q_t$  by a maximum of 0.65%. This similarity makes sense in the context of the Christchurch SCPTu sites, which as discussed in [1], are predominantly composed of soils with  $I_c$  values in the clean to silty sand behaviour type zone where pore pressure readings are typically small (i.e.,  $q_c \approx q_t$ ). Given the similarity in results shown by Fig. 3, it is evident that for the considered soils, either  $q_c$  or  $q_t$  can be used in the correlation without significantly changing performance. The raw tip resistance may be used for non-piezcone data or for piezcone data with questionable (or highly uncertain) pore pressure data, as well as for cases where the cone specifications needed to compute  $q_t$  are unavailable. The pore pressure corrected resistance can be used in all other appropriate cases. The model equations and the plots in this paper and in [1] are shown in terms of  $q_c$  for consistency of presentation. Based on the evaluations made during this discussion, the chosen regression functional form is defined as (with  $q_c$  as the tip resistance term):

$$V_s = a q_c^b f_s^d z^e \quad (9)$$

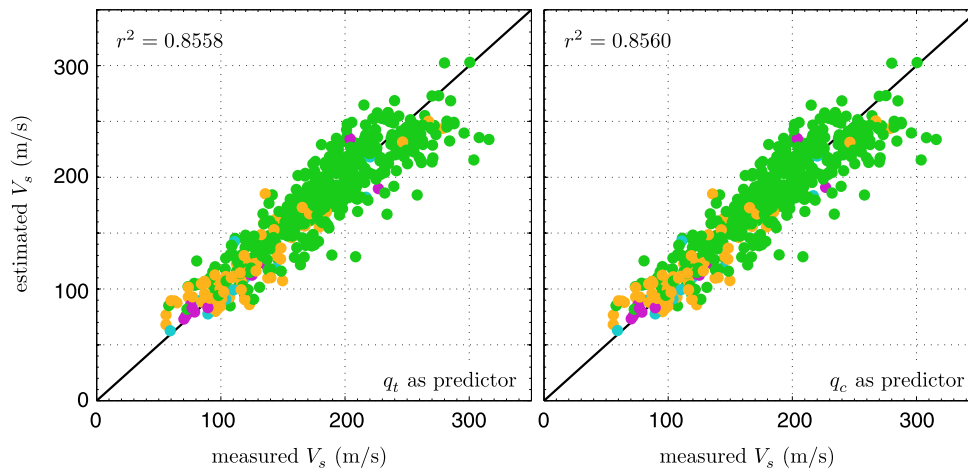


**Fig. 3.** Comparison of estimated and measured  $V_s$  for regression forms that consider corrected and raw cone tip resistance ( $q_t$  and  $q_c$ , respectively) as indicated. Marker colour indicates  $L_c$  as noted in Fig. 1. (For interpretation of the references to colour in this figure caption, the reader is referred to the web version of this paper.)

This regression equation is based entirely on terms directly measured by the CPT ( $q_c$ ,  $f_s$ , and  $z$ ). These terms are the least uncertain quantities that can be considered in the regression function, and this study has shown that the quality of the regression to the considered Christchurch-specific data set is not significantly different when consideration is given to these directly measured terms.

### 3. Consideration for non-constant conditional variance

Fig. 4 summarizes the performance of the regression form given by Eq. (9) when applied to the Christchurch SCPTu database. As indicated by the moving average trend lines (solid black lines), the residuals for this correlation are relatively consistent across the considered ranges of CPT-based variables, though it is evident from the depth variation plot that there is some variance in the data set with changes in  $z$ , as the data points are more spread out and confidence intervals (dashed black lines) are wider for shallow locations. As discussed in further detail in McGann et al. [1], there are several potential reasons for the larger bias at shallow depths, including: the averaging approach used to compare the unequal CPT and  $V_s$  measurement intervals (i.e., potentially greater variability in soil composition, and CPT readings, near the surface); the difference in the inclination of the path travelled by the shear waves emanating from the source for shallow and deep locations; and the increased uncertainty in the shallow CPT measurements due to lack of confinement. During the existing correlation evaluation study discussed in McGann et al. [1], the suitability of the shallowest data points was assessed by considering comparisons with and without the data points with  $z < 3$  m. It was determined that these points did not appear to unduly influence the overall bias of the comparisons, thus they were retained in the data set.

As indicated in the upper left-hand plot of Fig. 4, the presented results correspond to a regression analysis that considers constant conditional variance, hence constant conditional standard deviation,  $s_{y|x}$ , with depth (and all other predictor variables). These results imply that consideration for a conditional variance that is non-constant with depth in the regression analysis could lead to an improved prediction of shear wave velocity. Fig. 5 presents the performance of the regression with consideration for a non-constant conditional variance that varies with depth in the manner shown in the corresponding upper left-hand plot. Based on an examination of the residuals, it was determined that the depth is the only predictor variable from Eq. (9) with which there

was an apparent non-constant variance. As shown for  $s_{y|x}$  in the upper left plot of Fig. 5, a piecewise linear variation of variance with depth was considered as this was the simplest model appropriate for this purpose given the trends in the data. The depths at which the piecewise variance function changes slope ( $z = 5$  m and  $z = 10$  m) were manually chosen from a number of different depth ranges based on their effect on the regression results.

For the non-constant conditional variance model, the spread in the residuals evident in Fig. 4 at shallow depths becomes less pronounced and the overall distribution of the residuals with depth becomes more consistent in Fig. 5 (consistent in the sense that the distribution of the residuals is more even across the full range of depths in Fig. 5 as compared to Fig. 4). Because shallow depths typically correspond with lower shear wave velocities, the non-constant variance regression analysis naturally results in a tighter distribution of residuals at the lower ranges of the estimated  $V_s$  plot as well. Based on visual comparison of Figs. 4 and 5, the non-constant variance regression model produces more consistent residual distributions for all considered CPT-based variables. Though the confidence intervals for the moving average trend line are somewhat wider at deeper locations ( $z \geq 10$  m) in the non-constant variance case, this model yields a smaller standard deviation ( $s_{y|x} = 0.108$ ) than the constant variance model ( $s_{y|x} = 0.136$ ) in addition to the more consistent residual distributions evident in Fig. 5.

### 4. Final CPT- $V_s$ model

#### 4.1. Model equations

The Christchurch-specific CPT- $V_s$  correlation is determined from multiple linear regression in natural log space using the non-constant variance distribution and functional form, Eq. (9), discussed in the previous sections. The recommended best-fit equation for predicting  $V_s$  from CPT data in the non-surficial gravel portions of the of the shallow Christchurch and Springston Formations [43] is

$$V_s = 18.4q_c^{0.144}f_s^{0.0832}z^{0.278} \quad (10)$$

where  $q_c$  and  $f_s$  (units of kPa) are the raw cone tip and frictional resistances, respectively,  $z$  is the depth below the ground surface in metres, and  $V_s$  is the shear wave velocity in units of metres per second. Due to the near identical nature of  $q_c$  and  $q_t$  on average for the applicable soils (see Fig. 3), the pore pressure corrected tip



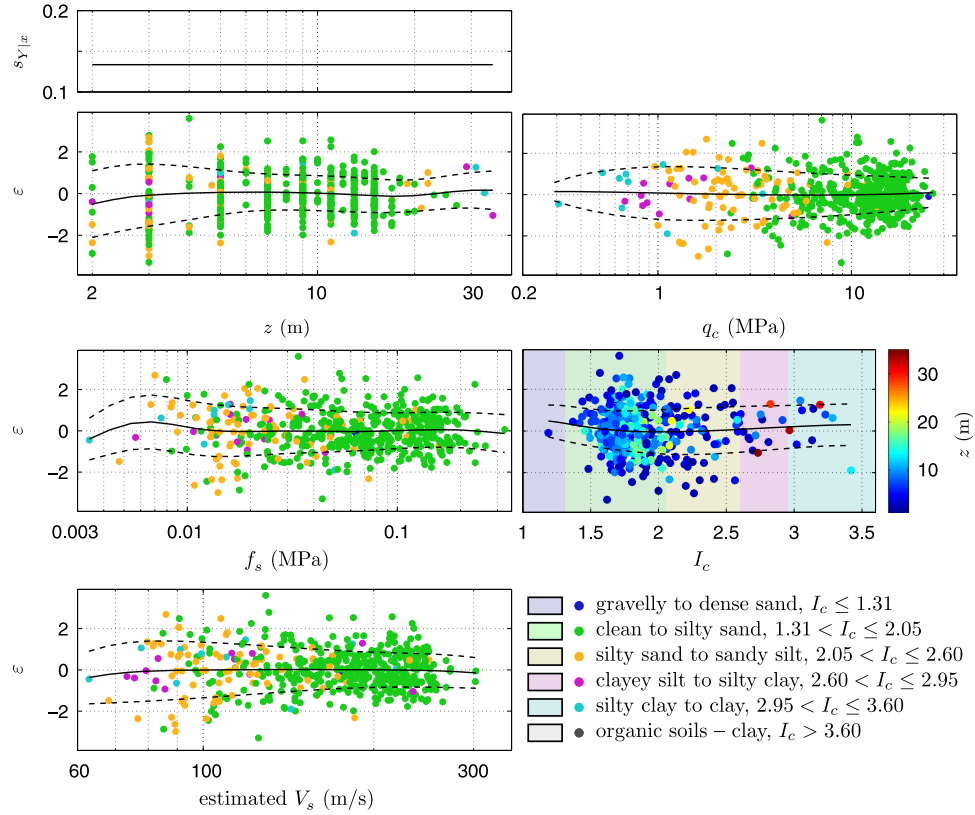


**Fig. 4.** Variation of residuals with  $z$ ,  $q_c$ ,  $f_s$ ,  $I_c$ , and estimated  $V_s$  for multiple linear regression, using functional form of Eq. (9), with constant variance for all predictor variables. Marker colour indicates soil behaviour type index,  $I_c$ , (or depth,  $z$ , in the  $I_c$  subplot) as noted. (For interpretation of the references to colour in this figure caption, the reader is referred to the web version of this paper.)

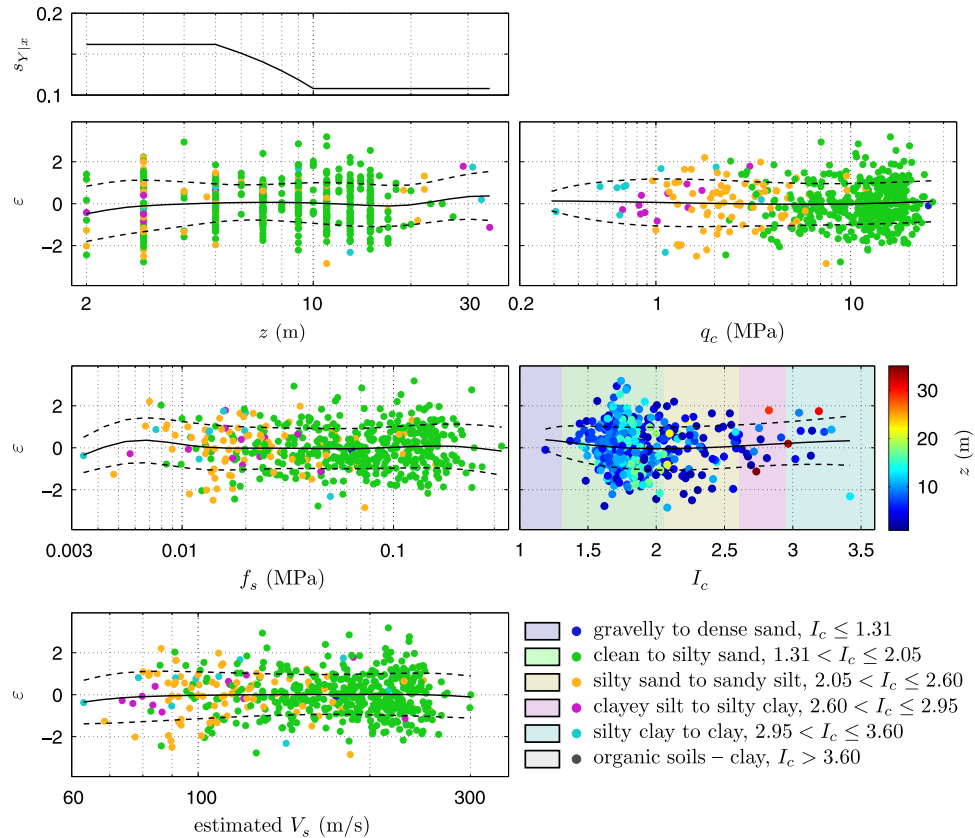


**Fig. 5.** Variation of residuals with  $z$ ,  $q_c$ ,  $f_s$ ,  $I_c$ , and estimated  $V_s$  for multiple linear regression (using functional form of Eq. (9)) with non-constant depth variance. Marker colour indicates soil behaviour type index,  $I_c$ , (or depth,  $z$ , in the  $I_c$  subplot) as noted. (For interpretation of the references to colour in this figure caption, the reader is referred to the web version of this paper.)

resistance ( $q_c$ ) may be used in place of  $q_c$  without change in the regression constants or performance. The piecewise standard deviation for the regression model is given by

$$\sigma_{\ln(V_s)} = \begin{cases} 0.162 & \text{for } z \leq 5 \text{ m} \\ 0.216 - 0.0108z & \text{for } 5 \text{ m} < z < 10 \text{ m} \\ 0.108 & \text{for } z \geq 10 \text{ m} \end{cases} \quad (11)$$

from which the prediction of  $V_s$  for a given percentile can be obtained as

$$V_{sx} = V_{s50} \exp(z_x \sigma_{\ln(V_s)}) \quad (12)$$

where  $x$  is the desired percentile,  $V_{s50}$  is the median prediction given by Eq. (10), and  $z_x$  is the standard normal variate for the  $x$ th percentile (e.g.  $z_x = 0, 1$  for the 50th and 84th percentiles, respectively). As shown by the plots of Fig. 5, the regression model of Eq. (10) produces consistent estimates of  $V_s$  across the full ranges of depth, cone and frictional resistance, and  $I_c$  soil behaviour type represented in the database, as well as for the full range of estimated  $V_s$  values returned by the correlation.

Support for the validity of the employed regression approach is provided by Fig. 6, which compares the cumulative probability distribution (CDF) for the analytical lognormal distribution with the CDF of the residuals,  $\varepsilon$ , for the empirical correlation computed using Eq. (7). The shown similarity between the empirical and theoretical cumulative distributions indicates that the data are lognormally distributed with respect to the prediction equation, providing confirmation that the normality assumption in the regression model, i.e.,  $\ln(V_s) = f(\ln(q_c), \ln(f_s), \ln(z))$ , is appropriate for the data set.

Fig. 7 shows the variation of the residuals with the factor of safety against liquefaction,  $FS_{liq}$ , computed using the method of Idriss and Boulanger [45] for each data pair. As discussed in

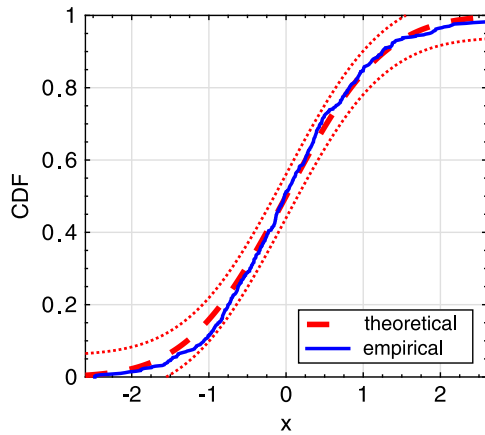


Fig. 6. Comparison of CDFs for empirical residuals and analytical lognormal distribution. Dotted lines represent Kolmogorov-Smirnov goodness-of-fit bounds [44] for  $\alpha=0.05$ .

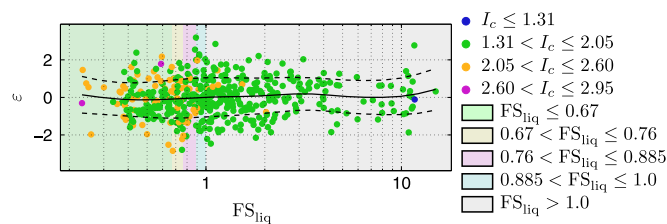


Fig. 7. Variation of residuals with estimated  $FS_{liq}$ , for multiple linear regression with non-constant depth variance. Marker colour indicates  $I_c$  as indicated in Fig. 1. Background colour indicates liquefaction likelihood class [1,46]. (For interpretation of the references to colour in this figure caption, the reader is referred to the web version of this paper.)

McGann et al. [1], the  $FS_{liq}$  of the considered soils was used to assess the potential reduction or loss of natural  $V_s$  increase with time due to the accumulation of age effects. In this context, lower  $FS_{liq}$  values are generally indicative of disturbed sites that may have lost age effects due to the 2010–2011 Canterbury earthquakes, and higher  $FS_{liq}$  values (larger than about 2.0) generally indicate that the age effects may be undisturbed. The background colours in Fig. 7 correspond to the likelihood of liquefaction classes of Taylor [46] (summarized in [1]), while marker colour corresponds to the soil behaviour type index. When the plotted  $FS_{liq}$  are interpreted as an indicator of apparent soil age as discussed in McGann et al. [1], Fig. 7 essentially indicates that the Christchurch-specific CPT- $V_s$  correlation given by Eq. (10) performs equally well for the full range of liquefaction histories and apparent ages in the current data set.

#### 4.2. Comparisons with specific SCPTu profiles

Figs. 8–11 compare  $V_s$  profiles estimated using the Christchurch-specific CPT- $V_s$  correlation of Eq. (10) with the measured  $V_s$  profiles for four sites in the Christchurch SCPTu database. The central solid line in the  $V_s$  plots of Figs. 8–11 defines the median estimated profile ( $V_{s50}$ ), while the shaded region bounded by dashed lines indicates the shear wave velocities at  $\pm$  one standard deviation from the solid line (i.e.,  $V_{s16}$  and  $V_{s84}$  from Eq. (12). McGann et al. [39] provide similar plots for the full set of 86 SCPTu sites. The white circular markers representing the measured  $V_s$  values are plotted at the center of the typically 2 m thick measurement intervals used in the SCPTu soundings. The solid vertical lines associated with each marker indicate the thickness of the measurement intervals over which the measured  $V_s$  values are assumed to be constant.

The sites shown in Figs. 8–11 were selected to demonstrate the ability of the current regression model to handle a variety of soil behaviour types and soil stiffness conditions. Figs. 8 and 9 represent relatively stiff (higher  $q_c$ ) soil sites that have the general behaviour types of a reasonably clean sand and a silty sand, respectively. Figs. 10 and 11 are representative of relatively soft (lower  $q_c$ ) soil sites with the same two respective general soil behaviour types (clean and silty sand). As shown, the measured and estimated  $V_s$  profiles appear visually similar for all four site conditions, and the measured  $V_s$  values generally fall within one standard deviation from the median prediction for each site.

#### 4.3. Model forward prediction using representative profiles

To demonstrate and assess the performance of the Christchurch-specific CPT- $V_s$  correlation in a purely forward prediction, as opposed to the comparisons of prediction and observation given by Figs. 8–11, six synthetic CPT profiles are generated and the regression model is applied to predict  $V_s$ . These synthetic profiles are based on three soil behaviour type cases: a clean sand ( $I_c = 1.55$ ), a silty sand ( $I_c = 1.95$ ), and a sandy silt ( $I_c = 2.45$ ). Fig. 12 shows the synthetic profiles and corresponding  $V_s$  profile predictions for each considered case. Two  $q_c$  profiles are assumed for each  $I_c$  case, one which represents a softer version of each soil behaviour type, and one which represents a stiff version. The chosen  $I_c$  and  $q_c$  values are informed by the distributions of these terms within the Christchurch SCPTu database [1] ( $q_c$  is used to avoid the assumption of penetration pore pressure distributions necessary to compute  $q_t$ ).

In order to apply the regression model to these synthetic profiles,  $f_s$  values are computed from the  $I_c$  equation of [36] for each combination of  $q_c$ ,  $I_c$ , and depth  $z$ . The soft-soil  $q_c$  values for each  $I_c$  case are approximately equal to the smallest values possible without requiring a negative frictional resistance. As

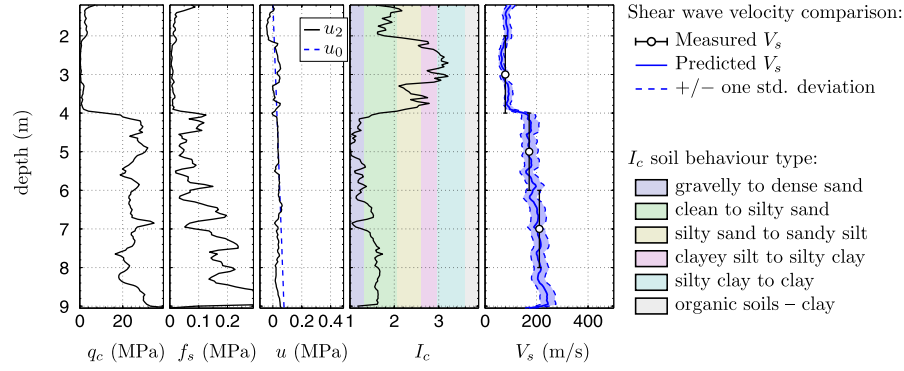


**Fig. 8.** Comparison of measured  $V_s$  values with Christchurch-specific CPT- $V_s$  estimated profile for site KAS46, representative of a clean sand (lower  $I_c$ ) soil site (for  $z > 4$  m) with stiff (higher  $q_c$ ) response. The groundwater table at this site was reported at 1.0 m depth.

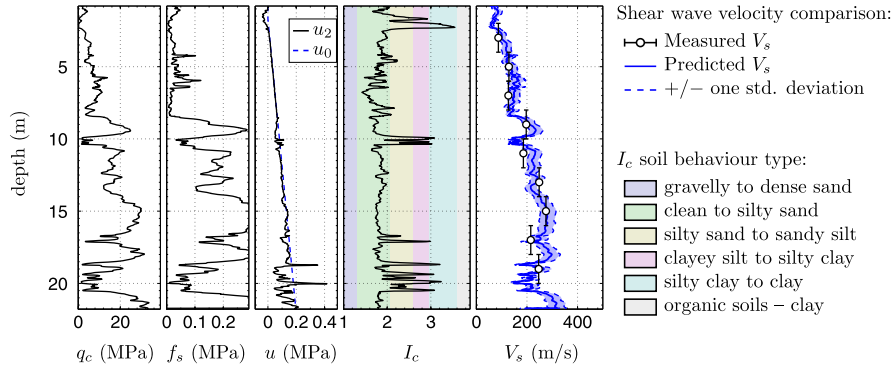


**Fig. 9.** Comparison of measured  $V_s$  values with Christchurch-specific CPT- $V_s$  estimated profile for site WAI14, representative of a silty sand (higher  $I_c$ ) soil site with stiff (higher  $q_c$ ) response. The groundwater table at this site was reported at 1.7 m depth.

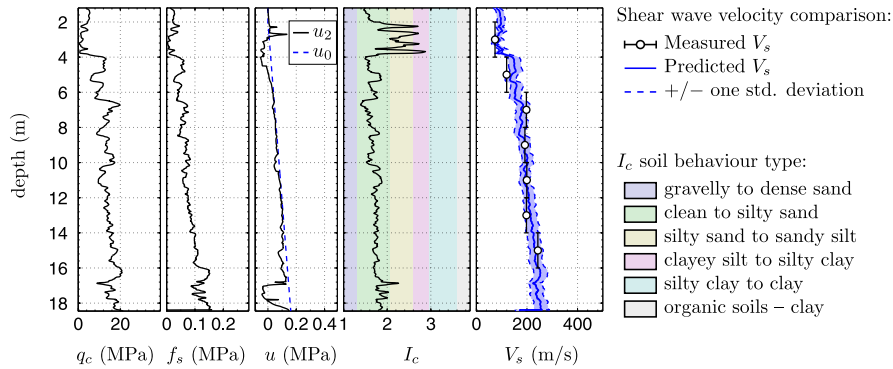


**Fig. 10.** Comparison of measured  $V_s$  values with Christchurch-specific CPT- $V_s$  estimated profile for site ARN28, representative of a sand (lower  $I_c$ ) soil site (for  $z > 4$  m) with soft (lower  $q_c$ ) response. The groundwater table at this site was reported at 2.0 m depth.

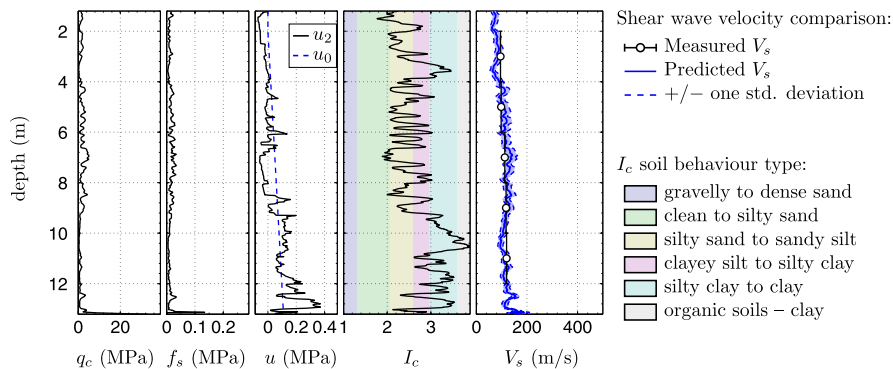


**Fig. 11.** Comparison of measured  $V_s$  values with Christchurch-specific CPT- $V_s$  estimated profile for site BDL08, representative of a siltier (higher  $I_c$ ) soil site with soft (lower  $q_c$ ) response. The groundwater table at this site was reported at 2.0 m depth.



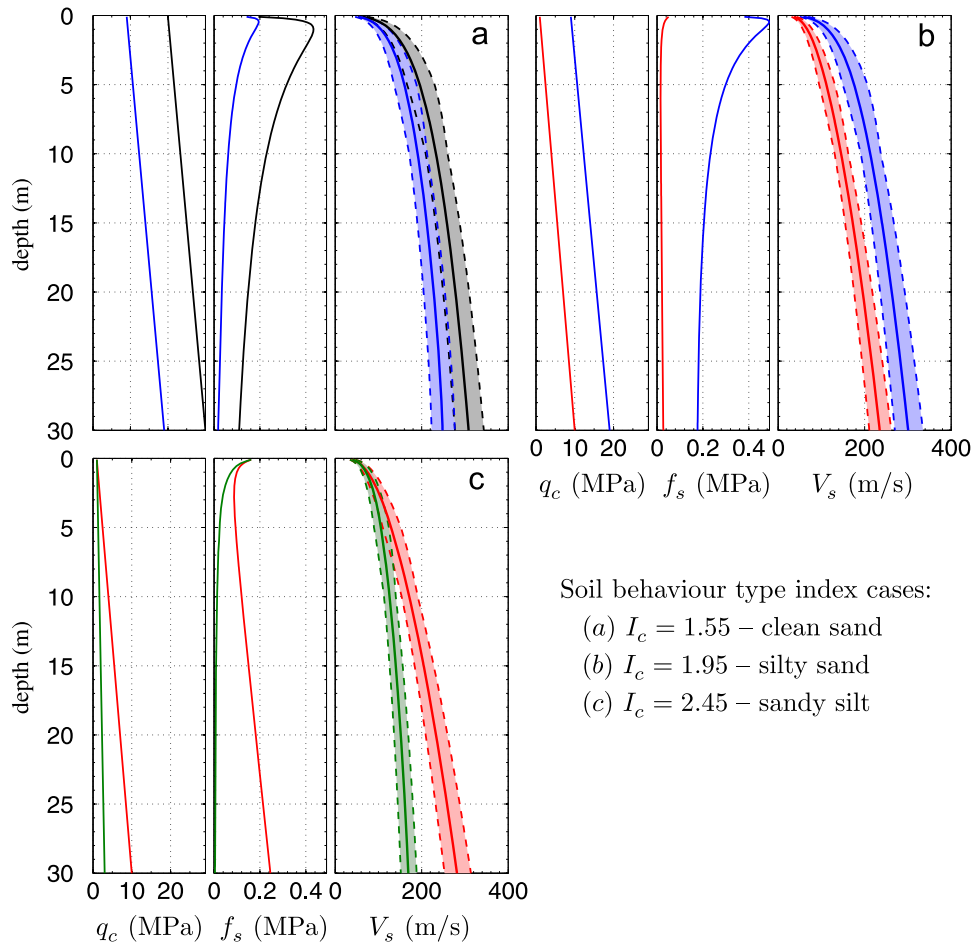


**Fig. 12.** Estimated  $V_s$  for synthetic soft and stiff CPT profiles based on the three indicated  $I_c$  cases. Solid lines in  $V_s$  plots are median predictions. Dashed lines indicate  $\pm$  one standard deviation from median.

shown in Fig. 12, the  $V_s$  predictions generally appear to be appropriately sensitive to changes in the predictor variables. Increasing the soil stiffness (via an increase in  $q_c$ ) for a given soil behaviour type results in higher shear wave velocities with depth. Due to the manner in which the soft soil profiles (lower  $q_c$ ) were defined, they hold a consistent relationship with  $I_c$  over the three considered soil behaviour type indices that does not apply to the stiff soil profiles. Comparison of these soft soil profiles across the three soil behaviour type cases shows that increasing  $I_c$  generally leads to a decrease in  $V_s$  for a given depth. Overall, the performance of the regression model is consistent with expectations in all of the considered synthetic forward prediction cases.

## 5. Conclusions

Multiple linear regression analysis was used to develop a CPT– $V_s$  relationship for Christchurch, New Zealand soils of the shallow Christchurch and Springston Formations [43] using the SCPTu database discussed in McGann et al. [1]. The selected regression equation depends on the raw cone tip and frictional resistances measured via the CPT,  $q_c$  and  $f_s$ , respectively, and the depth,  $z$  below the ground surface. The regression analysis considers non-constant variance with depth to create a correlation that returns consistent residuals with variations in the predictor variables, as well as with the estimated shear wave velocity and CPT-based soil behaviour type index. The new CPT– $V_s$  correlation provides a viable method to estimate  $V_s$  from CPT data that is specific to the non-gravel soils of the Christchurch and Springston

Formations within the study area in their current (i.e., post 2010–2011 earthquake sequence) state. Caution is suggested when applying the new CPT– $V_s$  correlation to sites located in the western portions of the Springston Formation where the SCPTu data are sparse (see McGann et al. [1], Fig. 1).

As part of the recovery effort following the 2010–2011 earthquakes in Christchurch, much effort has been made to characterize the near-surface soils of the region for such purposes as residential site classification, liquefaction susceptibility assessment, and other practical and research-related evaluations. As a result, there is a large, spatially dense database of CPT records for Christchurch city and the surrounding suburbs most affected by the earthquakes. In combination with the empirical CPT– $V_s$  prediction equation developed in this paper, this abundance of CPT data presents a unique opportunity for a region-wide estimate of the near-surface  $V_s$  profile of the soils in Christchurch, as well as the opportunity for site-specific  $V_s$  estimates anywhere there is a CPT record. Such site-specific and region-wide  $V_s$  characterizations should prove useful in future research efforts to evaluate near-surface site effects via site response analysis and to better understand the spatial variability in the shear wave velocity (and small strain shear modulus) of the near-surface soils of the region.

The ongoing earthquake recovery and research efforts in Christchurch have also resulted in a wealth of  $V_s$  measurement data obtained independently of the SCPTu database used in this study using various borehole-based [15–17] and surface-wave analysis techniques [8]. Using some of these available data, McGann et al. [47] show that the Christchurch-specific CPT– $V_s$  correlation compares favourably with  $V_s$  profiles measured using

surface-wave analysis methods at several Christchurch strong motion stations. In addition to the previously mentioned benefits of the new correlation, agreement between measured and estimated  $V_s$  values presents the potential for improved site-specific shear wave velocity characterization through the combination of directly measured and CPT-estimated  $V_s$  profiles. Because the CPT provides a nearly continuous variation of resistance data with depth, the  $V_s$  profile obtained from the Christchurch-specific CPT– $V_s$  correlation is also nearly continuous. This increased resolution can aid in refining the locations of layer boundaries where large velocity contrasts occur for measurement techniques with relatively coarse measurement resolution (e.g. surface-wave analysis), and result in improved inputs for site response analyses where the location of large impedance contrasts is a critical factor in defining the overall response of the system.

## Acknowledgements

Funding for this work was provided by the New Zealand Earthquake Commission (EQC) and the Natural Hazards Research Platform (NHRP). The authors would also like to thank the Canterbury Geotechnical Database and Perry Drilling Ltd. for providing data used in this study.

## References

- [1] McGann C, Bradley B, Taylor M, Wotherspoon L, Cubrinovski M. Applicability of existing empirical shear wave velocity correlations to seismic cone penetration test data in Christchurch New Zealand. *Soil Dyn Earthq Eng* 2015;75:76–86.
- [2] Bradley B. Ground motions observed in the Darfield and Christchurch earthquakes and the importance of local site response effects. *NZ J Geol Geophys* 2012;55(3):279–86.
- [3] Montalva G. Site-specific seismic hazard analyses [Ph.D. dissertation]. Washington State University; 2010.
- [4] Rodriguez-Marek A, Montalva G, Cotton F, Bonilla F. Analysis of single-station standard deviation using the KiK-net data. *Bull Seismol Soc Am* 2011;101:1242–58.
- [5] Bazzurro P, Cornell C. Nonlinear soil-site effects in probabilistic seismic-hazard analysis. *Bull Seismol Soc Am* 2004;94(6):2110–23.
- [6] Idriss I, Seed H. Soil moduli and damping factors for dynamic response analysis. Report EERC 70-10. University of California, Berkeley; 1970.
- [7] Darendeli M. Development of a new family of normalized modulus reduction and damping curves [Ph.D. dissertation]. University of Texas, Austin, TX, USA; 2001.
- [8] Stokoe II K, Santamarina J. Seismic-wave-based testing in geotechnical engineering. In: Proceedings of the international conference on geotechnical and geological engineering, GeoEng 2000. Melbourne, Australia; 2000. p. 1490–536.
- [9] Nazarian S, Stokoe II K. In-situ shear wave velocities from spectral analysis of surface wave tests. In: Proceedings of the 8th world conference on earthquake engineering. San Francisco, CA; 1984. p. 31–8.
- [10] Park C, Miller R, Xia J. Multichannel analysis of surface waves. *Geophysics* 1999;64(3):800–80.
- [11] Louie J. Faster, better shear wave velocity to 100 meters depth from refraction microtremor arrays. *Bull Seismol Soc Am* 2001;91(2):347–64.
- [12] Park C, Miller R. Roadside passive multichannel analysis of surface waves (MASW). *J Environ Eng Geophys* 2008;13(1):1–13.
- [13] Tokimatsu K, Shinzawa K, Kuwayama S. Use of short-period microtremors for  $V_s$  profiling. *J Geotech Eng* 1992;118(10):1544–58.
- [14] Okada H. The microtremor survey method [Suto K, Trans.]. In: SEG geophysical monograph series no. 12. Society of Exploration Geophysicists; Tulsa, OK; 2003.
- [15] Woods R. Measurement of dynamic soil properties, state of the art report. In: Proceedings of the ASCE specialty conference on earthquake engineering & soil dynamics; vol. 1. Pasadena, USA: California Institute of Technology; 1978. p. 91–178.
- [16] Woods R. Borehole methods in shallow seismic exploration. In: Woods R, editor. Geophysical characterization of sites. ISSMFE Technical Committee #10. New Delhi, India; 1994. p. 91–100.
- [17] Kaneko F, Kanemori T, Tonouchi K. Low-frequency shear wave logging in unconsolidated formations for geotechnical applications. In: Paillet F, Saunders W, editors. Geophysical applications for geotechnical investigations. ASTM STP 1101. Philadelphia, PA, USA: American Society for Testing and Materials; 1990. p. 79–98.
- [18] Ohta Y, Goto N. Empirical shear wave velocity equations in terms of characteristic soil indexes. *Earthq Eng Struct Dyn* 1978;6(2):167–87.
- [19] Sykora D, Stokoe II K. Correlations of in-situ measurements in sands and shear wave velocity. Geotechnical Engineering Report GR83-33. The University of Texas at Austin; 1983.
- [20] Rollins K, Evans M, Diehl N, Daily W. Shear modulus and damping relationships for gravels. *J Geotech Geoenviron Eng* 1998;124(5):396–405.
- [21] Wair B, DeJong J, Shantz T. Guidelines for estimation of shear wave velocity profiles. PEER Report No. 2012/08. Pacific Earthquake Engineering Research Center, University of California, Berkeley; 2012.
- [22] Andrus R, Mohanan N, Piratheepan P, Ellis B, Holzer T. Predicting shear-wave velocity from cone penetration resistance. In: Proceedings of the 4th international conference on earthquake geotechnical engineering. Paper No. 1454. Thessaloniki, Greece; June 25–28, 2007.
- [23] Hegazy Y, Mayne P. A global statistical correlation between shear wave velocity and cone penetration data. In: Puppala A, Fratta D, Alshibli K, Pamukcu S, editors. Proceedings of the GeoShanghai, site and geomaterial characterization (GSP 149). Reston, VA: ASCE; 2006. p. 243–8.
- [24] Robertson P. Interpretation of cone penetration tests—a unified approach. *Can Geotech J* 2009;46(11):1337–55.
- [25] Baldi G, Bellotti R, Ghionna V, Jamiolkowski M, Lo Presti D. Modulus of sands from CPTs and DMTs. In: Proceedings of the 12th international conference on soil mechanics and foundation engineering, vol. 1. Rio de Janeiro; Balkema Publishers, Rotterdam; 1989. p. 165–70.
- [26] Mayne P, Rix G.  $G_{max}$ – $V_s$  relationships for clays. *Geotech Test J* 1993;16(1):54–60.
- [27] Hegazy Y, Mayne P. Statistical correlations between  $V_s$  and cone penetration data for different soil types. In: Proceedings of CPT'95, vol. 2. Linköping, Sweden: Swedish Geotechnical Society; 1995. p. 173–8.
- [28] Tarantola A. Inverse problem theory and methods for model parameter estimation. Philadelphia, PA, USA: Society for Industrial and Applied Mathematics (SIAM); 2005.
- [29] Xia J, Miller R, Park C. Estimation of near-surface shear-wave velocity by inversion of Rayleigh waves. *Geophysics* 1999;64(3):691–700.
- [30] Bradley B, Cubrinovski M. Near-source strong ground motions observed in the 22 February 2011 Christchurch earthquake. *Seismol Res Lett* 2011;82(6):853–65.
- [31] Bradley B. Strong ground motion characteristics observed in the 4 September 2010 Darfield, New Zealand earthquake. *Soil Dyn Earthq Eng* 2012;42:32–46.
- [32] Cubrinovski M, Bradley B, Wotherspoon L, Green R, Bray J, Wood C, et al. Geotechnical aspects of the 22 February 2011 Christchurch earthquake. *Bull NZ Soc Earthq Eng* 2011;44(4):205–26.
- [33] Cubrinovski M, Bray J, Taylor M, Giorgini S, Bradley B, Wotherspoon L, et al. Soil liquefaction effects in the central business district during the February 2011 Christchurch earthquake. *Seismol Res Lett* 2011;82(6):893–904.
- [34] Cubrinovski M, Green R, Allen J, Ashford S, Bowman E, Bradley B, et al. Geotechnical reconnaissance of the 2010 Darfield (Canterbury) earthquake. *Bull NZ Soc Earthq Eng* 2010;43(4):243–320.
- [35] Campanella R, Gillespie D, Robertson P. Pore pressures during cone penetration testing. In: Proceedings of the 2nd European symposium on penetration testing, ESPT II. Amsterdam; May 24–27, 1982. p. 507–12.
- [36] Robertson P, (Fear) Wride C. Evaluation cyclic liquefaction potential using the cone penetration test. *Can Geotech J* 1998;35(3):442–59.
- [37] Zhang G, Robertson P, Brachman R. Estimating liquefaction-induced ground settlements from CPT for level ground. *Can Geotech J* 2002;39(5):1168–80.
- [38] Ang AS, Tang W. Probability concepts in engineering emphasis on applications to civil and environmental engineering. 2nd ed. Hoboken, NJ, USA: John Wiley & Sons, Inc.; 2007.
- [39] McGann C, Bradley B, Cubrinovski M, Taylor M, Wotherspoon L. Development and evaluation of CPT– $V_s$  correlation for Canterbury New Zealand soils of the shallow Christchurch and Springston Formations. University of Canterbury Research Report No. 2014-01; 2014.
- [40] Wasserman L. All of nonparametric statistics. Secaucus, NJ, USA: Springer-Verlag New York, Inc.; 2006.
- [41] Jefferies M, Davies M. Soil classification by the cone penetration test: discussion. *Can Geotech J* 1991;28(1):173–6.
- [42] Robertson P. Soil behaviour type from the CPT: an update. In: 2nd international symposium on cone penetration testing, CPT'10. Paper No. 2-56. Huntington Beach, CA; May 9–11, 2010.
- [43] Brown L, Weeber J. Geology of the Christchurch urban area. Lower Hutt, New Zealand: Institute of Geological and Nuclear Sciences Ltd.; 1992.
- [44] Massey Jr F. The Kolmogorov–Smirnov test for goodness of fit. *J Am Stat Assoc* 1951;46(253):68–78.
- [45] Idriss I, Boulanger R. Soil liquefaction during earthquakes, MNO-12. Earthquake Engineering Research Institute (EERI); Oakland, CA; 2008.
- [46] Taylor M. The geotechnical characterisation of Christchurch sands for advanced soil modelling [Ph.D. dissertation]. University of Canterbury, Christchurch, New Zealand; 2014.
- [47] McGann C, Bradley B, Wotherspoon L, Cox B. Comparison of a Christchurch-specific CPT– $V_s$  correlation and  $V_s$  derived from surface wave analysis for strong motion station velocity characterization. *Bull NZ Soc Earthq Eng* 48(2), 2015.